SUMMARY OF MICHIGAN MULTISPECTRAL INVESTIGATIONS PROGRAM

by

Richard R. Legault
Willow Run Laboratories
The University of Michigan
Ann Arbor, Michigan

INTRODUCTION

This paper is a summary of the NASA supported activities at The University of Michigan's Willow Run Laboratories in the area of multispectral remote sensing. The objectives of this program are to improve and extend the techniques for multispectral recognitions of remotely sensed objects. The program has two major areas of activity. The first is a series of investigations directed in improving the techniques; the second is a series of programs with various users to extend the usefulness of these techniques and to show their practical application. In this paper, I shall summarize the activities of the past year in the development of multispectral techniques. The paper following will discuss the exploitation of the techniques developed in previous years, as well as those developed in this last year.

The primary thrust of last year's activities has been the development of techniques to extend spectral signatures in space and time. The fundamental barrier to the multispectral signature extension has been variations in the environment. These variations are differences, both spatially and temporally, in atmospheric transmission, illumination of the scene, and backscatter components. In previous years we pointed out that there are three ways one may hope to obtain such signature extensions. The first is by making suitable transformations on the remotely collected multispectral data; the intent of these transformations is to make the data invariant despite variations in transmission, illumination and backscatter. The second possible method is to employ ancillary sensors in the data collection platform which, in fact, do measure the illumination, transmission and backscatter. An example of such an ancillary sensor is the sun sensor now flown in the Michigan C47 aircraft. The third technique is to select in-scene references, which provide a calibration or reference source in the scene that permit us to correct the data.

The second area of effort has been the development of data upon which spectral signatures can be based. The data referred to here is laboratory data of the spectral reflectance and transmission of various materials. In addition, models of various types of problems have been constructed and, as we shall show later, are exploited to investigate various problems in remote sensing. This effort has resulted in the compilation of data and methods for retrieving this data for the remote sensing community as a whole.

The third effort has been the development of techniques which show some promise of enabling us to determine the composition of spatially unresolved scene elements. We shall treat the subject in fair detail later.

The fourth area of effort has been an investigation of the problems of multispectral data processing. Our attention has been directed towards practical speeds for such computations. We shall treat this subject in some detail as it has been a matter of some discussion in past meetings. This discussion has centered around the relative merits of digital and analog computation in the past. We will show that, in fact, both techniques have their place in an operational system.

Finally, some attention has been paid to problems of multispectral instrumentation. We shall not discuss the work we have done in this area in this paper.

Twelve reports will be issued on the work of this past year. During the course of the summary, I shall refer to these reports so that those interested in more detail than we have time to present here can have the required reference.

SIGNATURE EXTENSION

Spectral signatures are obtained today in the following manner. The objects to be recognized are identified in image form and from these areas the statistics for defining the spectral signatures are obtained. The problem at present is that the signatures obtained in this fashion usually do not hold for areas very far distant from the original learning set or for times very much different than the original collection time. A consequence of this is that a considerable amount of ground truth has to be collected in order to make effective use of spectral recognition techniques. Despite this rather obvious shortcoming, spectral recognition has played a role and undoubtedly will continue to do so, but perfection of the technique will require methods which allow us to extend the signature in both space and time. Equation (1) presents the rather unusual expression for the signal in the i^{th} spectral channel obtained by a multispectral remote sensor.

$$S(\lambda_i, \theta) = [H(\lambda_i)\tau(\lambda_i, \theta)\rho(\lambda_i, \theta) + b(\lambda_i, \theta)]K_i \qquad (1)$$

where $S(\lambda_i,\theta)$ = signal from instrument
λ_i = spectral interval
θ = parameters of observation, direction, and distance
$H(\lambda_i)$ = irradiance (direct and diffuse sunlight)
$\tau(\lambda_i,\theta)$ = transmission
$\rho(\lambda_i,\theta)$ = material reflectance
$b(\lambda_i,\theta)$ = backscatter
K_i = instrument response

The term that carries the information about the material in the expression is of course the reflectance of the material, $\rho(\lambda_i,\theta)$ and it is variation in this reflectance from one material to another that permits an identification. One is all too well aware, however, that we may expect variations in the irradiance or illumination $H(\lambda)$, transmission or visibility $\tau(\lambda)$ and in the backscatter component $b(\lambda)$. These variations of illumination, transmission and backscatter are a primary source for the variation of the remotely sensed spectral signature and are a major contributor to the dilemma we face today in terms of signature extension.

That illumination, transmission and backscatter should vary from one area to another or from one time to another is not surprising, and considering that our present method for processing the data is to accept these variations, it is again not surprising that we have difficulty in establishing spectral signatures that will hold for very large areas or for very long periods of time.

One method for obtaining a spectral signature that is, in fact, invariant under variations in these environmental factors of illumination, transmission, and backscatter, is the transformation of the remotely sensed spectral data to obtain a new set of values which are hopefully invariant. Last year, we reported on some of the ratioing or normalizing transformations and illustrated their success under certain circumstances. Tabulated below are some of the multispectral transformations that we have tried.

$$\frac{S(\lambda_1,\theta)}{S(\lambda_2,\theta)} \cdots\cdots, \frac{S(\lambda_{11},\theta)}{S(\lambda_{12},\theta)}$$

$$\frac{S(\lambda_2,\theta)}{S(\lambda_1,\theta)} \cdots\cdots, \frac{S(\lambda_{12},\theta)}{S(\lambda_{11},\theta)}$$

$$\frac{S(\lambda_2,\theta) - S(\lambda_1,\theta)}{S(\lambda_2,\theta) + S(\lambda_1,\theta)} \cdots\cdots, \frac{S(\lambda_{12},\theta) - S(\lambda_{11},\theta)}{S(\lambda_{12},\theta) + S(\lambda_{11},\theta)}$$

The reader is referred to Reference 1 to see some of the successes that were obtained. Now, these transformations essentially assume that we can ignore the backscatter component. They further assume that the ratio of illumination and transmission for two adjacent channels is essentially a constant.

$$\frac{H(\lambda_i)\tau(\lambda_i,\theta)}{H(\lambda_{i+1})\tau(\lambda_{i+1},\theta)}$$

The above expression is a constant for all atmospheric conditions and for all wavelengths. These techniques have been partially successful. In our view, the major failure of these techniques has been in their inability to adequately compensate for variations in the angles of observation.

These angular effects are illustrated in Figures 1, 2 and 3. In Figure 1, we have a video print of scanner data of Colorado grassland. Figure 2 is a three dimensional representation of the signal amplitude for a scanner strip of this area in the 0.4 to 0.44 μm regions; in Figure 3 a similar strip of the same area is shown in the 0.8 to 1 μm band. The reader can get a rough impression of the general slope or angular dependence by looking at the latter two figures. It should be apparent that the angular effects are, in fact, wavelength dependent by comparing the two figures. The very prominent dip in both of these figures is a cloud shadow,and in Figure 4 we will show a rather interesting method for detecting cloud shadows in the imagery.

In Figures 2 and 3, the horizontal dimension represents the flight path and the vertical dimension represents the scan dimension and is denoted in subsequent descriptions of the scan angle variations. If one looks closely at this data, one sees that if we average over local variations, a fairly well defined scan angle variation is sensible. This correction factor for scan angle is essentially obtained by averaging in the flight path dimension for a fixed scan angle and fixed spectral interval. This averaging process is represented in equation (2) below:

$$f(\lambda_i,\theta) = \frac{1}{T}\int_0^T S(\lambda_i,\theta,T)dT \qquad (2)$$

where T = flight path dimension

θ = scan angle

The primary question, of course, is the interval over which such averaging should take place; in other words, how long a path length T should we take for finally determining the value of $f(\lambda_i)$ for a fixed value of θ. The inverse of the correction function $f(\lambda_i,\theta)$ is then used to correct the remotely sensed data for angular effects. This technique is fairly obviously a combination of the transformed techniques discussed

earlier as well as the employment of in-scene references. In the particular scene in which this has been exploited so far, the various different elements have been randomly scattered with respect to the scan angle. Thus, we have a fairly unbiased estimate of the angular effects exploiting this averaging. Reference 1 covers in more detail this technique and some of the other work on transformation techniques that we have done during the past year, and reference 2 discusses the application of that technique to some actual data. The second paper will cover in more detail the results of this exploitation of the technique.

Figure 4 is a ratio of the 0.4 to 0.44 μm bands to the 0.8 to 1 μm band. It is rather interesting to note that the cloud shadow becomes very obvious in this ratio presentation. The reason I think is fairly clear, that the cloud shadow is relatively darker in the 0.8 to 1 μm band than it is in the 0.4 to 0.44 μm band, the difference largely due to the fact that the short wavelength 0.4 to 0.44 μm band is primarily direct sunlight. The identification of cloud shadows and the subsequent correction of the data for cloud shadows detected in this manner is another way to extend the spectral signatures.

A second method for extending the spectral signatures is to employ ancillary sensors in the remote sensor platform to measure illumination, transmission and backscatter. At the present time, the Michigan C47 aircraft carries a sun sensor which measures the total downward irradiance at the aperture of the sun sensor. We have found that normalization of the remotely sensed multispectral data by the sun sensor data collected in each channel during the dead time of the scan has enabled us to extend the spectral signatures significantly. However, the simple normalization techniques have not accomplished all that we might desire. Consequently, we have initiated investigations into the calculation of the signals received by various types of sun sensors and the relationship to the backscatter, transmission and ground irradiance or illumination values. Figures 5 and 6 are the results of some of these calculations for albedos at the ground plane of 0. Figure 5 shows computations for visibility range of 23 km and Figure 6 for visibility range of 2 km, a quite significant difference in the atmospheric conditions.

The first impression that one receives in looking at this data is the fact that the total downward radiation which is currently being measured by our sun sensor is not nearly as sensitive to variations in the atmospheric conditions as is the diffuse downward component. This is hardly surprising since the diffuse component as measured from the aircraft platform (provided it is well within the atmosphere) should, in fact, be a fair measure of the atmospheric conditions. The real test of the importance of this is seen in the following tabulation.

	Visibility	
	2 km	23 km
Diffuse Sun Sensor	42	24
Total Sun Sensor	186	185
Total Ground H(.55)	168	178
Backscatter b(.55)	9	5
Transmittance	.23	.83
$H(\lambda)\tau(\lambda)$	38.6	148.7

Sun Sensor Estimates of Illumination and Transmittance

Here we have assumed the sensor platform is flying at 2 km and have tabulated the signal in milliwatts per square meter per micrometer for a diffuse sun sensor, the total sun sensor, the illumination of the ground plane in the 0.55 μm band, the backscatter and the transmittance. The factor that we really have to consider is in fact not the total illumination of the ground plane or the transmittance separately, but the product of the two, the last line in the above tabulation, and it is apparent that the variations in the signal received by the diffuse sun sensor under the two visibility or atmospheric conditions described is much closer to defining the variability that we see in the product of transmittance and illumination $H(\lambda)\tau(\lambda)$. Both the diffuse and total sun sensors are inversely related to the product $H(\lambda)\tau(\lambda)$ and the diffuse sun sensor outputs are a fair representation of the backscatter component, while the total sun sensor signal is a fair representation of the total ground illumination $H(\lambda)$. However, if we were forced to use a single sun sensor output, and since the factor that we wish to eliminate is the product of transmittance and total ground illumination, we would be forced to use the diffuse sun sensor signal.

There is, of course, no need to limit ourselves to either the total or diffuse measurement. We have, in fact, incorporated into the C47 system a diffuse sun sensor along with the total sun sensor so that more adequate normalization procedures can be employed. We believe it is possible to develop correction factors exploiting the diffuse and total sun sensor signals to more accurately measure transmittance, backscatter and ground illumination than is done by simple normalization by the diffuse and total sun sensor signals. Our next task in this area is to develop these correction procedures.

SPECTRAL SIGNATURES

The basis for multispectral detection as we have noted before are variations in the reflectance and emittance of various materials. In order to define the data processing, it is desirable to have available the

reflectivities and emissivities of various materials so that the potential false alarms as well as detection probabilities may be calculated before expensive operational tests of the detection procedure are made. To this end, we have compiled the available spectral reflectance and emittance data; this data compilation is reported in reference 3. The spectral signature data has, in addition, been digitized and retrieval programs have been generated. This retrieval and analysis program is described in reference 4. The digitized data are also available to the remote sensing community from either Houston or The University of Michigan. The available spectral data are far from complete; the data gaps are identified in reference 5. It is our hope that the remote sensing community will collaborate with us in filling these gaps and we hope that this document will be of use to other organizations in planning their measurement programs.

We have in addition exploited this data to some newer applications for remote sensing techniques. As most of you are aware today, our operations are limited to the 0.32 to 1 μm region. In the very near future we shall have common aperture multispectral sensors from 0.32 to 14 μm and it seems very obvious that we should start considering the use of multispectral thermal or infrared data. Figure 7 is a composite plot of the emission spectra of various silicon dioxide based rocks. It is well known that the emissivity dip in the 9 to 10 μm region is due to the reststrahlen of silicon dioxide. The minimum of this reststrahlen dip for acidic rocks occurs at a shorter wavelength (roughly 9.4 μm) than does the minimum for ultra basic rocks (roughly 10.2 μm). It should then not be surprising that one might attempt to define the acidity of various rock types on the basis of multispectral data collected in the 9 to 11 μm region. Some manipulation of these data convinced us of the potential of this technique.

A recently developed laminar detector was made available to us. The top layer of this detector was sensitive in the 8.2 to 10.9 μm range and the bottom detector was sensitive in the 9.4 to 12.3 μm range. A brief glance convinces one that there is some hope that by taking the ratio of these two bands, the acidity of the rock type might be determined. While the spectral bands encompassed by this detector are not optimal for this task by any stretch of the imagination, it is the first common aperture multispectral data available to us in the 8 to 14 μm band.

In Figure 8 we show the images collected in the two bands respectively as well as the ratio. If the ratio of the 8.2 to 10 μm channel to the 9.4 to 12.1 μm channel is small, we would tend to say that acidic rock is present. In the ratio image of Figure 8, we see fairly dim areas around a silicate quartz sand quarry in Mill Creek, Arizona. In the two images separately, a body of water is noted in the lower central portion of the image. In the ratio image a dark outline for these areas indicates the sand shores of this body of water. Subsequently, Dr. Kenneth Watson of USGS and his colleagues have walked this area and identified all the

dark portions of this particular scene as being high acidic, silicon-dioxide-based rocks. While they have not investigated all the other portions of this scene, they have not found any other silicon-dioxide-based rocks that were not detected by this ratio technique. This work is reported in reference 6.

The spectral signatures work in the past year has also included some modeling of the radiation characteristics for various phenomena. One of the tasks undertaken was an attempt to determine whether ground water could be detected in thermal imagery. This work was in support of some data interpretation for the Columbia Basin area. There was some indication that thermal patterns in the scene were associated with varying depths of water table in this particular area. Consequently, calculations were made to determine whether the temperature as measured at the surface could be used as an indicator of the water table. The environmental conditions, relative humidity, temperature, time of the year and wind velocities for the period of data collection were used in these calculations. We used a one dimensional thermal model which allows us to assume various types of materials in layered structures.

In Figure 9 is plotted the diurnal cycle for temperature variations for two soil types. It should be noted that at certain times of the day, the differences of soil types do in fact produce different temperatures which would be detectable by an IR scanner. In Figure 10, different moisture contents for a single soil type were assumed and once again for optimal times of day detectable temperature differences are present.

In Figure 11, we considered a structure for the terrain with the water table at varying depths but with identical surface moistures and soil types. It is apparent that no detectable temperature differences for the environmental conditions postulated (in this particular example, they were in the late fall) are detectable. If underground water is going to be detected, it is likely that it will be by one of three means — either differences in vegetation types present at the surface where underground water is present, differences in soil moisture (which is very likely to occur), or differences in soil types probably related to permeability of the soil. While there still remains some hope for detection of underground water based upon remotely sensed infrared radiation, more work on the mechanism of such detection seems warranted at this time. It is also clear that both the time of day for this detection process and time of year will play an essential role.

DETECTION OF SPATIALLY UNRESOLVED OBJECTS

Much has been said to date of the problems associated with the limited spatial resolution capabilities of the first generation satellite-borne remote sensors. These remote sensors have concentrated on spectral coverage

rather than spatial coverage. That this concentration is warranted is partially demonstrated in the following work that was done during the last year. At first glance, it would seem impossible to identify objects that are spatially unresolved. This is certainly true if we are considering single spectral channel systems. However, the ability to measure the spectral distribution of radiance does offer us the possibility to resolve the elements within a resolution element -- in other words, the capability of identifying spatially unresolved objects. One example is the percent ground cover of an agricultural crop which is indicative of stage of growth and vigor. In Figure 12, we have such a classical problem, viz. the detection of the amount of weeds and bare soil in a corn field. Now let us consider this particular corn field as being a composite of corn plant reflectance spectra, the reflectance spectra of weeds and the reflectance spectra of bare soil. There is a certain percentage of each one of these pure types of materials in an individual resolution element. Very few sensors at almost any aircraft altitude are able to tell us very precisely what these percentages are. However, if we consider the multispectral signature of each individual type of materials (weeds, corn plant and soil) as vertices of a convex mixture, then the particular field we are looking at contains percentages of each of these types. In Figure 13, we have the reflectance spectra of bare soil and corn. These are pure spectral signatures of each of the materials. Now suppose a particular resolution element contains equal amounts of corn and bare soil while another resolution element contains 20% corn and 80% bare soil. We expect to see differences in the reflectance spectra for the various resolution elements and, in fact, we do as a scene in Figure 14. We are in fact able to take this composite spectrum and determine the percent of various elements that are within the resolution element.

A model for this detection is follows:

MODEL

Signature of Type i Material is Gaussian Distribution with Mean A_i and Covariance Matrix M_i. If Proportion of Type i Material in Mixture is X_i, Signature of Mixture Has Mean A_x and Covariance Matrix M_x Given by:

$$A_x = \sum_i X_i A_i$$

$$M_x = \sum_i X_i M_i$$

The procedure that we follow is to first identify the pure signatures that we expect to see in the resolution element. Of course, the expectation may not be realized for all of the elements, but they have to be sufficient in number to cover the possibilities that might be there. Secondly, we examine our data sample and estimate the proportions of each of the pure signatures that are present in the particular data sample representing the resolution element. The algorithms required for this estimation are developed and defined in reference 7 (along with some applications of the convex mixture algorithms to actual data). There is one practical problem in doing this work. At the present time, we have very little ground truth information which allows us to estimate the correct proportions of various materials within resolution elements or, for that matter, within various agricultural type fields. This lack of appropriate ground truth data for such things as percent ground cover has prohibited us from making very accurate tests of techniques developed. Hopefully within the coming year, such data will become available and we shall be in a position to properly validate the models. However, we have been able to obtain statistics from pure strains of various materials and simulate the statistics of these strains in such a way as to test out the validity of the convex mixture algorithm. Table I presents the results of such a simulation.

TABLE I. RESULTS OF ESTIMATING PROPORTIONS (SIMULATION)

Material	True Value of Proportion	Estimated Value of Proportion	Error
Sugar Beets	0.5500	0.5375	-0.0125
Weeds	0.2500	0.2397	-0.0103
Bare Soil	0.2000	0.2085	0.0085
Alfalfa	0.0000	0.0004	0.0004
Barley	0.0000	0.0139	0.0139

The basic data upon which the pure spectral signatures of sugar beets, weeds, bare soil, alfalfa and barley are based on data collected in the Imperial Valley during the spring of 1968. The simulation, therefore, is realistic in the sense that it is based upon actual data, but the proportions and the variations of the spectral signatures are the factor simulated. The results given in Table I are remarkably accurate. For example, the true proportion of sugar beets in our simulated area was 0.55, and we estimate 0.54. Such results are sufficiently encouraging to lead us to continue pursuing this work, particularly in light of the practical importance of developing such techniques for the first generation satellite remote sensors.

The only practical application of this technique made to date has been over a Colorado grasslands area where various nitrogen fertilizer treatments were applied. While once again we had inadequate ground truth to determine the percentages of tall, mid-length and short grasses on the various plots investigated, it was possible to at least quantitatively determine whether the algorithm was working properly. In Figure 1, we have a panchromatic image of the Colorado grassland area where the nitrogen treatments were applied. The treatments were applied at various times so that data was available on the height of the grass from the time of treatment. As we can see in Figure 15, the algorithm predicts more tall grass for the nitrogen treated plots than for plots receiving no treatments and that the rate of growth of the grass is greater for the nitrogen treated plots, as we might expect. In this particular case, we have specified percentages of the three grass heights that were involved. The best that we can say is that the results agree with what our intuition would be. As we have said before, there is no ground truth to support the results of these estimations. Various problems with the computational algorithms have been identified and work is currently going on to correct them. The technique will be exploited with more airborne data during the coming year.

DATA PROCESSING

Multispectral processing of remotely sensed data has proven effective in many applications related to earth resources studies. However, these applications usually require timely processing of large quantities of data and today this processing is several orders of magnitude beyond our capabilities. For example, if the U.S. and its coastal waters were overflown twice a year with presently planned equipment, the data collected would require a conventionally organized digital computer with a cycle time of 10^{-10} seconds to keep pace with the data collection rates. This cycle time is a factor of 10^4 faster than that obtainable with presently available digital computers. Alternative methods of computations are available. A parallel-channel, hard-wired analog computer system at The University of Michigan (SPARC) does in fact meet this data rate. However, there are drawbacks with this type of system. The set up of such an analog computer is extremely slow and its versatility is somewhat limited, whereas the digital computer is a much more versatile device. It seems, then, fairly clear that the type of operational data processing system that we will ultimately be led to combines the best features — program ability primarily of the digital computer, and the high throughput calculation rate of hard-wired, parallel-channel analog facilities.

During the past year, we have investigated the possible design alternatives for such a hybrid multispectral data processing facility. The results of these investigations are given in detail in references 8 and 9. Essentially these investigations began by considering some of the limitations

of the current analog systems. The major problems with the current analog systems are the time involved in setting up the problem for computation and the difficulty in optimizing the recognition procedure. It became fairly clear that an improved system should utilize a digital facility in the problem set up and the process optimization, and rely on the parallelism of the analog portion of the system for the bulk computation. Thus, we have a fairly standard hybrid where the digital computation system acts as a controller for the analog processor which does the high speed parallel channel computation.

In Figure 16, we have a component diagram for such a system which indicates the various types of units that are involved. We have data inputs and data primarily from magnetic tape, tape buffer storages, interfaces between both display and digital computer for the analog processor, preprocessor and the analog recognition processor. The recognition output is then interrogated by the digital system for determining whether it is operating according to plan. In Figure 17, we see the various functions that are performed and some estimate in terms of factors of real time for these various functions. The proposed hybrid system gives an effective reduction of a factor of 32 in the time for processing multispectral data. The type of equipment proposed here is, of course, prototype and there is little doubt that with more engineering work that hybrid facilities could, in fact, be designed to meet real time.

INSTRUMENTATION

During the past year, three small studies of multispectral instrumentation have been performed. The results of these investigations are given in references 10, 11 and 12. We shall not discuss these reports in any detail. Very briefly, we considered the utilization of detectors in line scanners, some optical transfer techniques for multispectral orbital scanners, and some problems of calibrating multispectral scanners. These problems had arisen during the design and fabrication of the 24-channel multispectral scanner for aircraft use and the 10-channel Skylab sensor. These studies were an integral part of the engineering support we furnished NASA, Houston during the fabrication of the 24-channel and Skylab sensors.

CONCLUSIONS

I should like to be able to report that our work on the spatial and temporal extension of multispectral signature had been completed. I cannot. A complicated multispectral recognition problem that required 219 learning sets last year can now be done with 13 learning sets. Signatures that were

valid for 30 miles last year have been extended for 129 miles using transformation and sun sensor data. But there are still cases where our techniques will not work. We have sorted out most of the problems of signature extension and expect next year to be able to define the limits of signature extension and how the extension should be attained.

Spectral reflectance and emittance data are now available to the remote sensing community. This data can be used to define the approach to many multispectral remote sensing problems. All too often multispectral recognition is based on spectral differences which appear in a set of remotely sensed data without our being able to explain why such differences should be present. Consequently, we are unable to state with any certainty whether the recognition experiment can be repeated. An explanation of the observed differences based on the optical properties of the materials gives us some confidence of the recognition experiment's repeatability. We hope that the successful use of signature data reported will persuade the remote sensing investigators to make more extensive use of such data.

The most exciting new development is the possibility of recognizing spatially unresolved scene elements using multispectral data. These techniques are in their infancy but show considerable promise. A new factor must now be considered when defining required spatial resolutions. If spatially unresolved elements can be identified in some cases using multispectral data, we should have a new look at the remote sensing problems requiring high spatial resolution to determine whether or not they can be solved with the new multispectral recognition techniques for unresolved spatial elements.

REFERENCES

1. STUDIES OF SPECTRAL DISCRIMINATION, W. A. Malila, R. Turner, R. Crane, C. Omarzu, Report No. 3165-22-T, in publication.

2. INVESTIGATIONS RELATED TO MULTISPECTRAL IMAGING SYSTEMS FOR REMOTE SENSING, J. Erickson, Report No. 3165-17-P, in publication.

3. THE NASA EARTH RESOURCES SPECTRAL INFORMATION SYSTEM: A DATA COMPILATION, V. Leeman, et.al., Report No. 3165-24-T, in publication.

4. EXPANDED RETRIEVAL ANALYSIS SYSTEM FOR THE NASA EARTH RESOURCES SPECTRAL INFORMATION SYSTEM, V. Leeman, et.al., Report No. 3165-22-T, in publication.

5. DATA GAPS IN THE NASA EARTH RESOURCES SPECTRAL INFORMATION SYSTEM, R. Vincent, Report No. 3165-25-T, in publication.

6. REMOTE SENSING DATA ANALYSIS PROJECTS ASSOCIATED WITH THE NASA EARTH RESOURCES SPECTRAL INFORMATION SYSTEM, R. Vincent, et.al., Report No. 3165-26-T, in publication.

7. INVESTIGATIONS OF MULTISPECTRAL SENSING OF CROPS, R. Nalepka, et.al., Report No. 3165-30-T, in publication.

8. A PROTOTYPE MULTISPECTRAL PROCESSOR WITH HIGH THROUGHPUT CAPABILITY, F. Kriegler, R. Marshall, Report No. 3165-23-T, in publication.

9. DATA PROCESSING DISPLAYS OF MULTISPECTRAL DATA, F. Kriegler, R. Marshall, Report No. 3165-28-T, in publication.

10. DETECTOR UTILIZATION IN LINE SCANNERS, Leo Larsen, Report No. 3165-29-T, in publication.

11. CALIBRATION OF MULTISPECTRAL SCANNERS, J. Braithwaite, Report No. 3165-27-L, in publication.

12. INVESTIGATION OF SHALLOW WATER FEATURES, F. Polcyn, et.al., Report No. 3165-31-T, in publication.

6

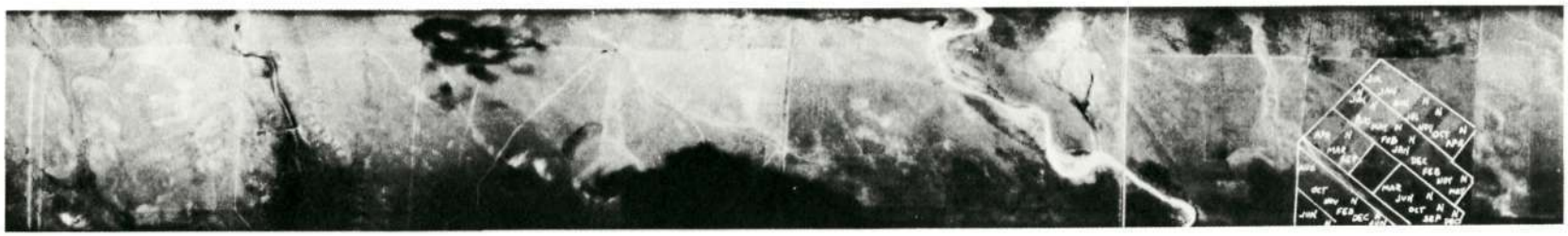

VIDEO PRINT OF SCANNER DATA FROM COLORADO GRASSLAND 0.62-0.66 μm.

INFRARED AND OPTICS LABORATORY
INSTITUTE OF SCIENCE AND TECHNOLOGY
WRL
THE UNIVERSITY OF MICHIGAN

Figure 1

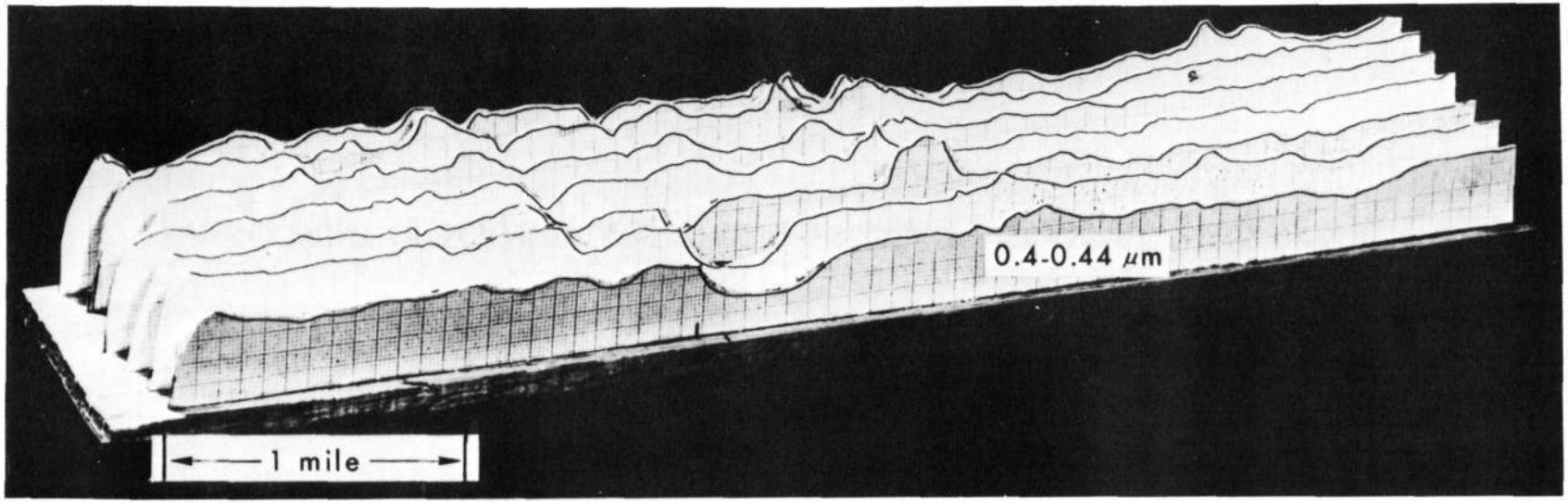

THREE DIMENSIONAL PLOT OF FILTERED SCANNER DATA FROM COLORADO GRASSLANDS, 0.4-0.44 μm

Figure 2

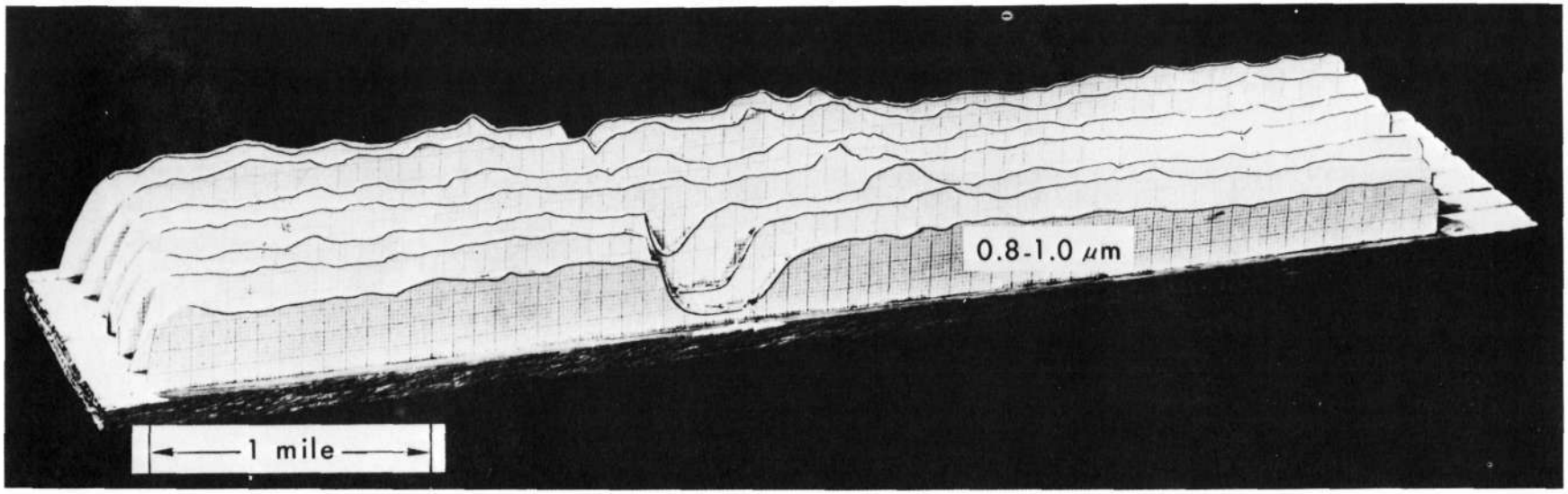

THREE DIMENSIONAL PLOT OF FILTERED SCANNER DATA FROM COLORADO GRASSLANDS, 0.8-1.0 μm

Figure 3

INFRARED AND OPTICS LABORATORY
INSTITUTE OF SCIENCE AND TECHNOLOGY
WRL
THE UNIVERSITY OF MICHIGAN

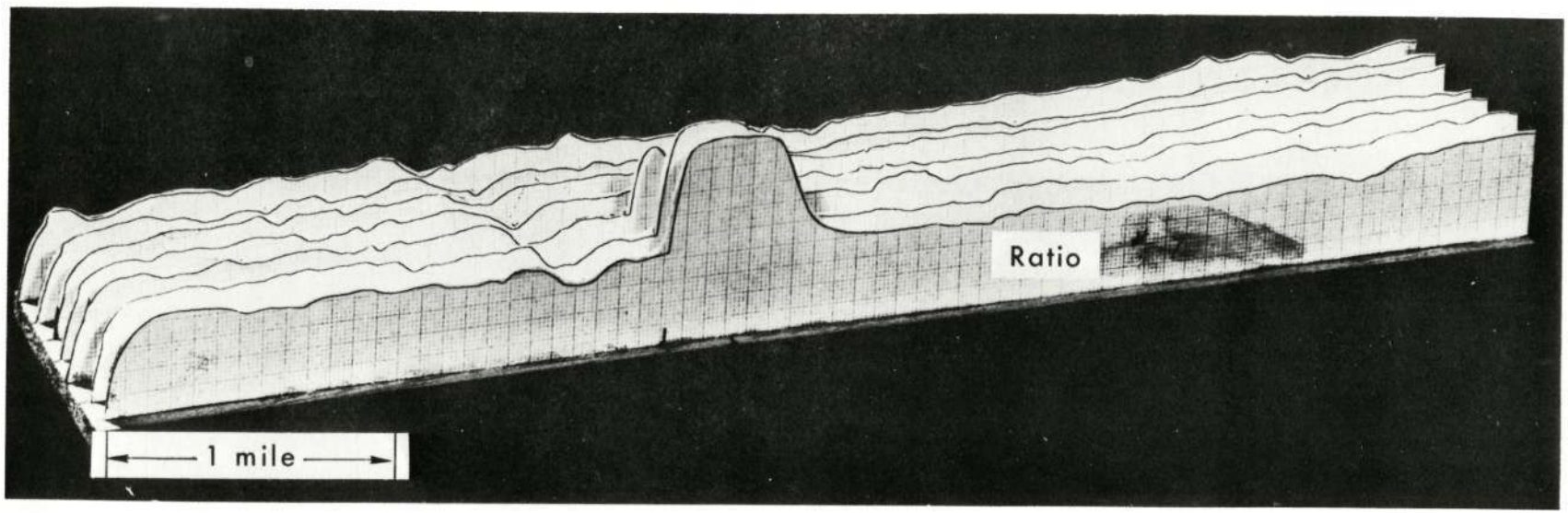

THREE DIMENSIONAL PLOT OF FILTERED VOLTAGE RATIO, $V_{\downarrow}0.4\text{-}0.44 / V_{\downarrow}0.8\text{-}1.0$, FROM COLORADO GRASSLANDS SCANNER DATA

Figure 4

INFRARED AND OPTICS LABORATORY
INSTITUTE OF SCIENCE AND TECHNOLOGY
WRL
THE UNIVERSITY OF MICHIGAN

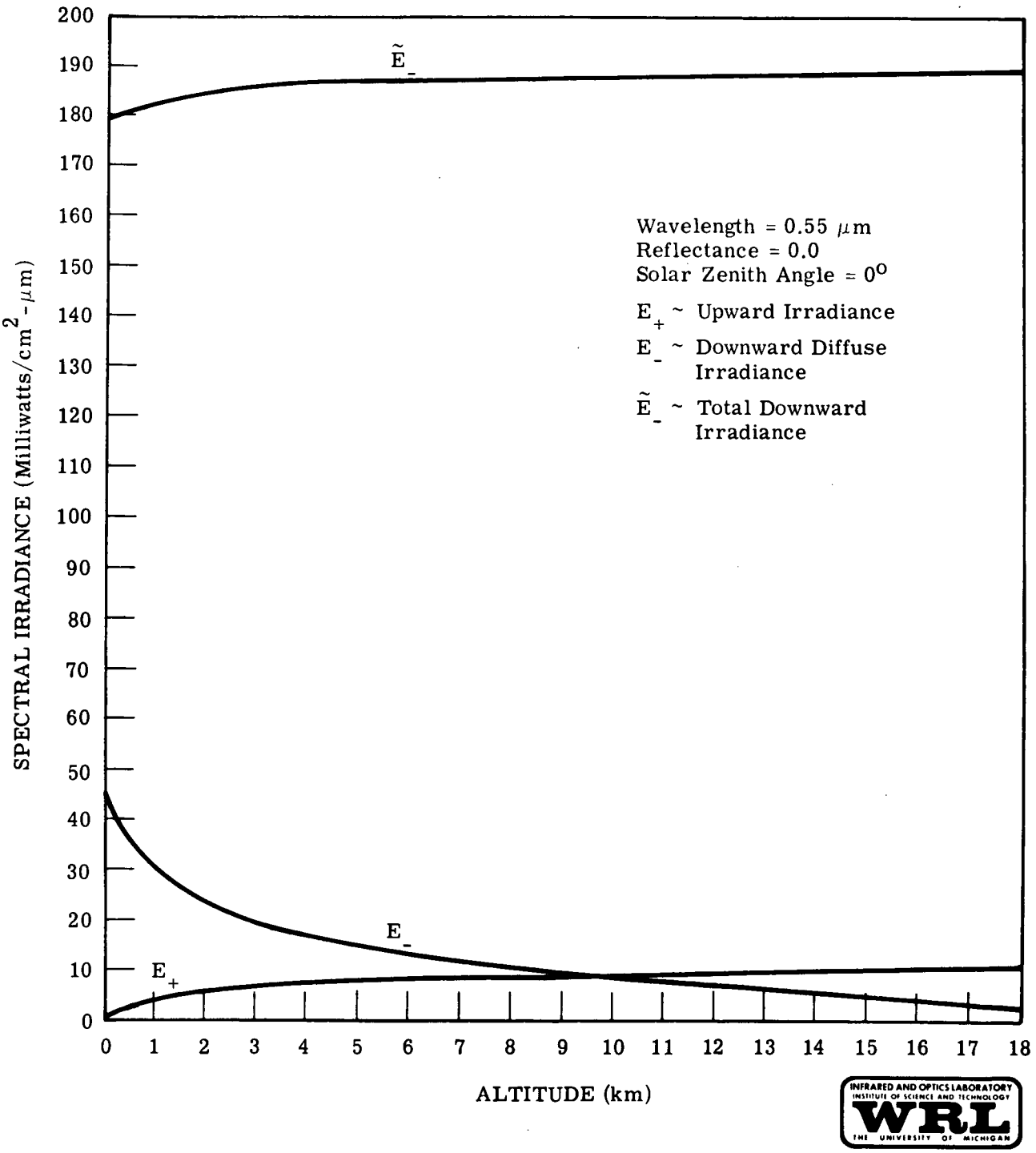

ALTITUDE DEPENDENCE OF IRRADIANCES IN A HOMOGENEOUS ATMOSPHERE WITH A VISIBILITY OF 23 km

Figure 5

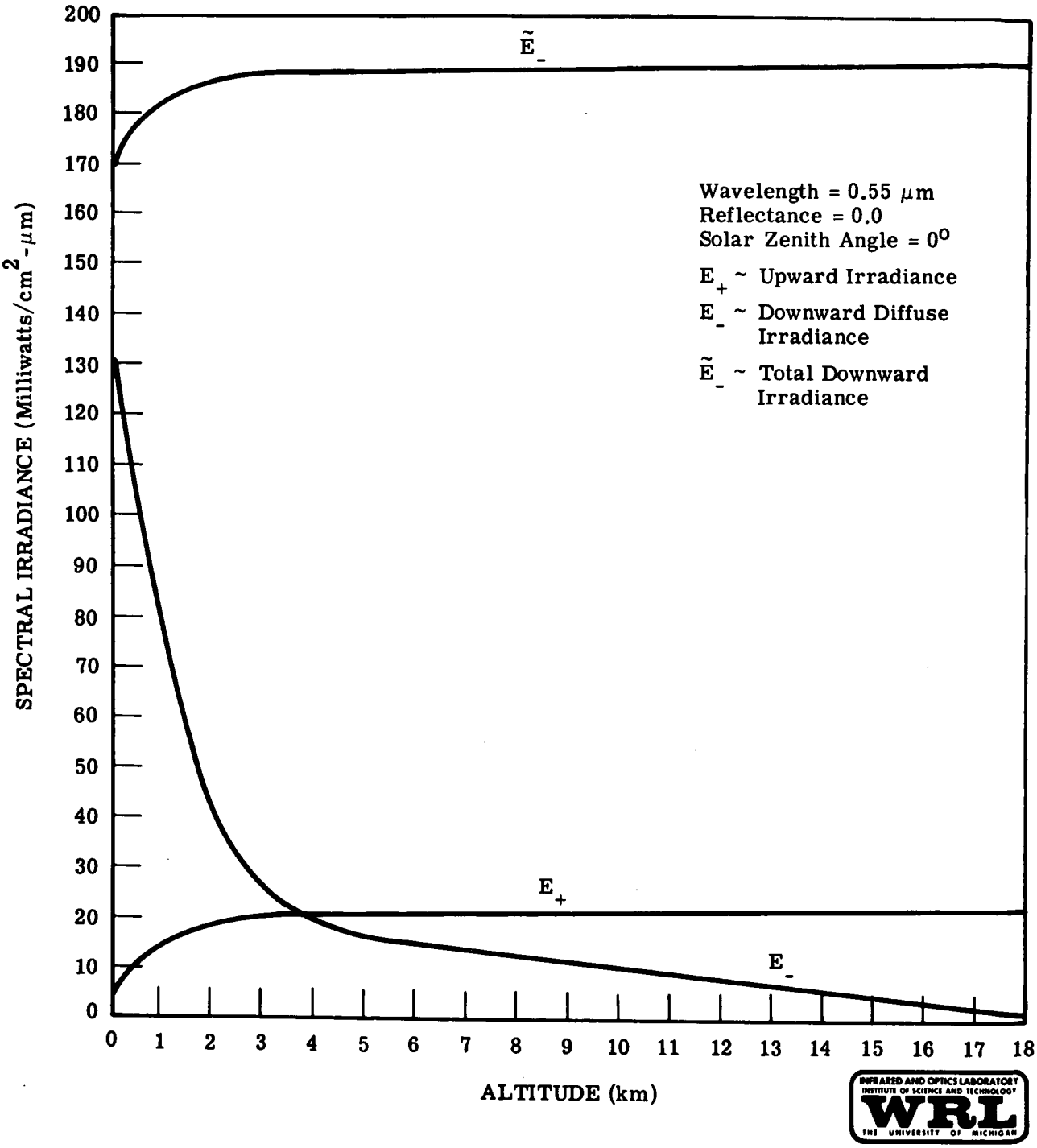

ALTITUDE DEPENDENCE OF IRRADIANCES IN A HOMOGENEOUS ATMOSPHERE WITH A VISIBILITY OF 2 km

Figure 6

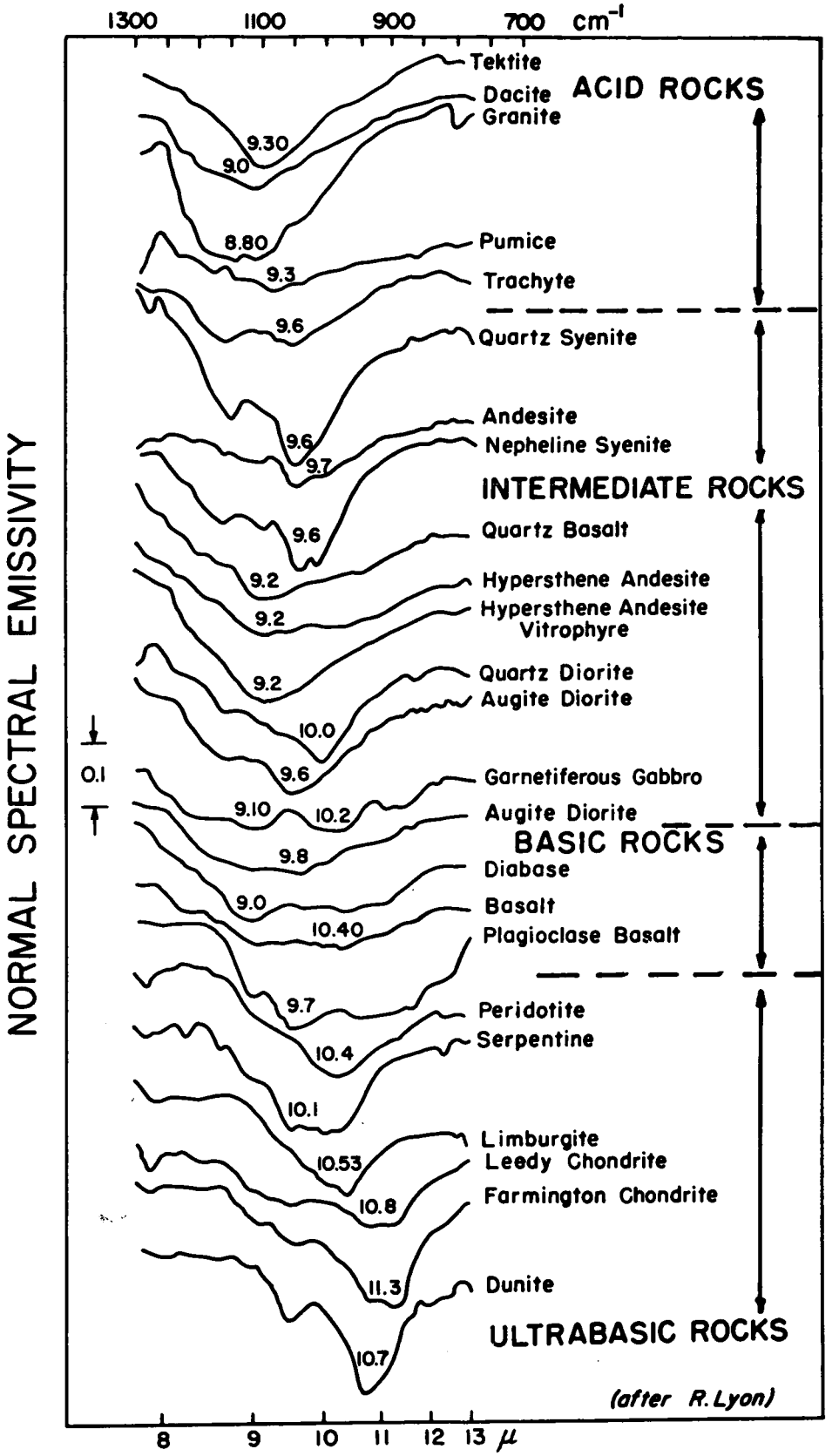
1300
1100
900
700
cm⁻¹
NORMAL SPECTRAL EMISSIVITY
0.1
Tektite
Dacite
Granite
ACID ROCKS
9.30
9.0
8.80
Pumice
9.3
Trachyte
9.6
Quartz Syenite
Andesite
9.6
9.7
Nepheline Syenite
INTERMEDIATE ROCKS
9.6
Quartz Basalt
9.2
Hypersthene Andesite
9.2
Hypersthene Andesite
Vitrophyre
9.2
Quartz Diorite
Augite Diorite
10.0
9.6
Garnetiferous Gabbro
9.10
10.2
Augite Diorite
BASIC ROCKS
9.8
Diabase
9.0
Basalt
10.40
Plagioclase Basalt
9.7
Peridotite
10.4
Serpentine
10.1
Limburgite
10.53
Leedy Chondrite
10.8
Farmington Chondrite
11.3
Dunite
ULTRABASIC ROCKS
10.7
(after R. Lyon)
8
9
10
11
12
13 μ

Figure 7

8.2-10.9 μm

9.4-12.1 μm

Ratio

DISCRIMINATION OF ACIDIC SILICATES NEAR MILL CREEK, OKLAHOMA
(Sand Quarry)

Figure 8

INFRARED AND OPTICS LABORATORY
INSTITUTE OF SCIENCE AND TECHNOLOGY
WRL
THE UNIVERSITY OF MICHIGAN

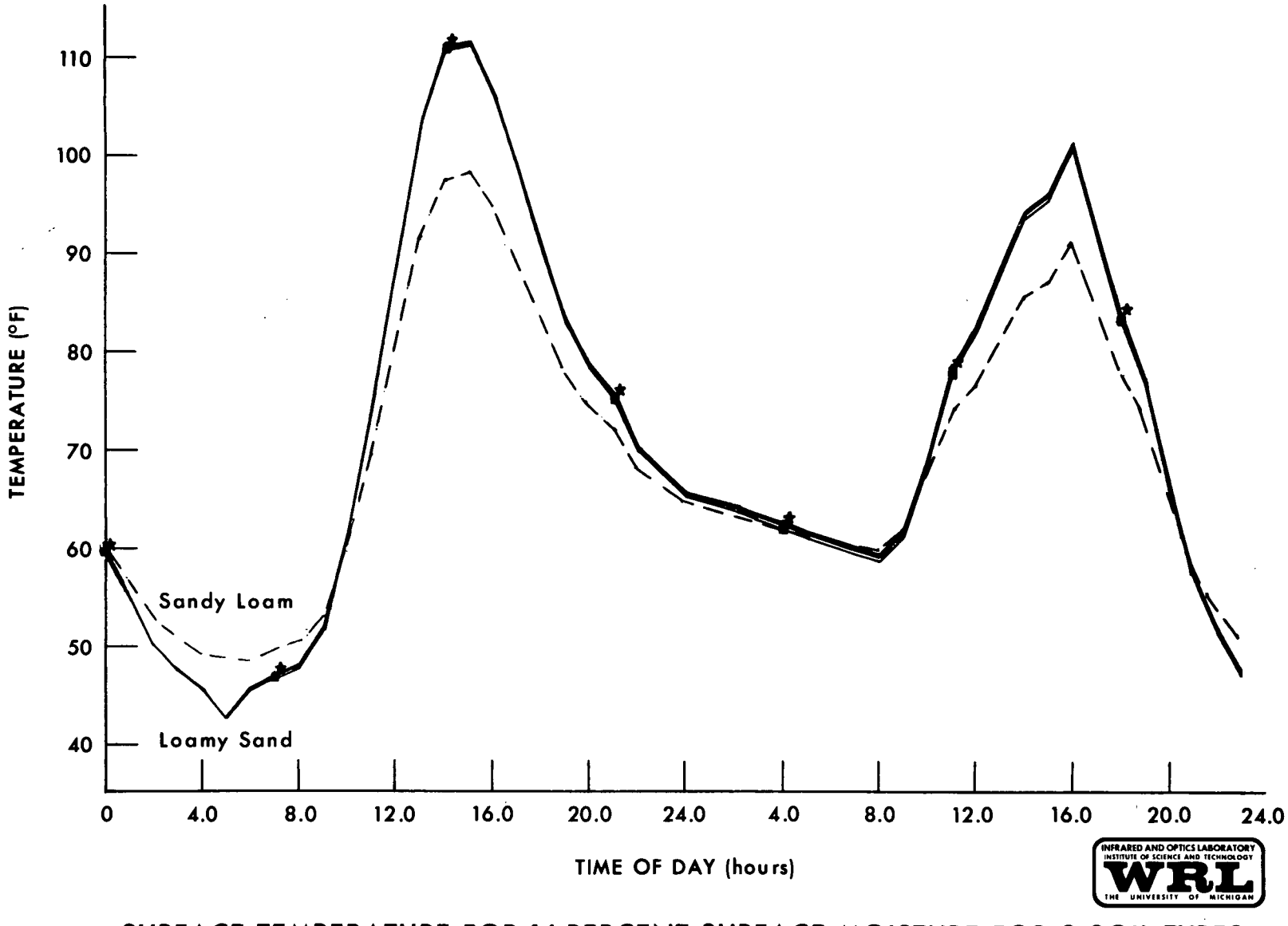

422

SURFACE TEMPERATURE FOR 16 PERCENT SURFACE MOISTURE FOR 2 SOIL TYPES

Columbia Basin Area

Figure 9

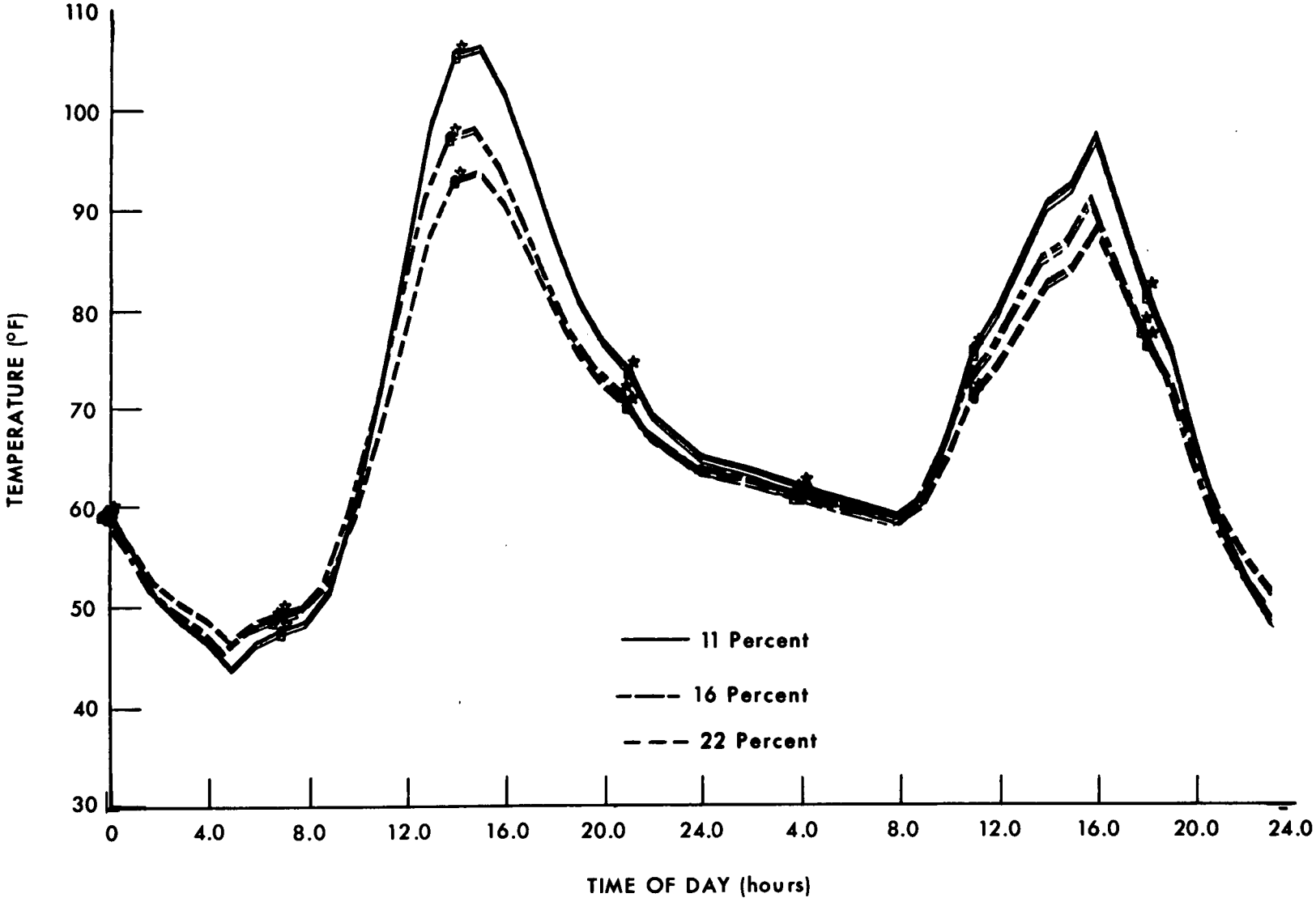

SURFACE TEMPERATURE FOR SANDY LOAM AT 3 DIFFERENT SURFACE MOISTURE PERCENTAGES

Columbia Basin Area

INFRARED AND OPTICS LABORATORY
INSTITUTE OF SCIENCE AND TECHNOLOGY
WRL
THE UNIVERSITY OF MICHIGAN

Figure 10

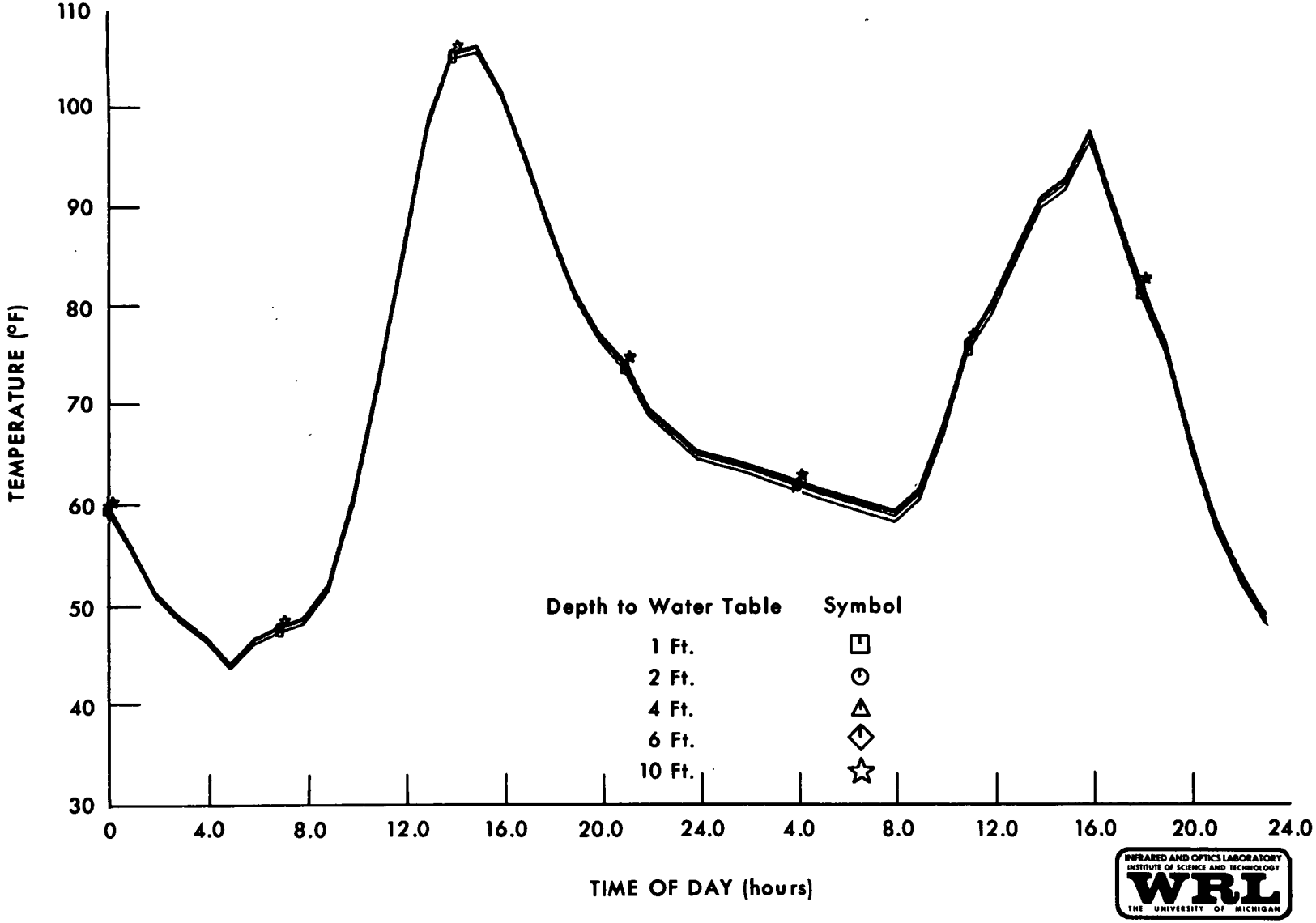

SURFACE TEMPERATURE FOR SANDY LOAM AT 11 PERCENT SURFACE MOISTURE

Columbia Basin Area

Figure 11

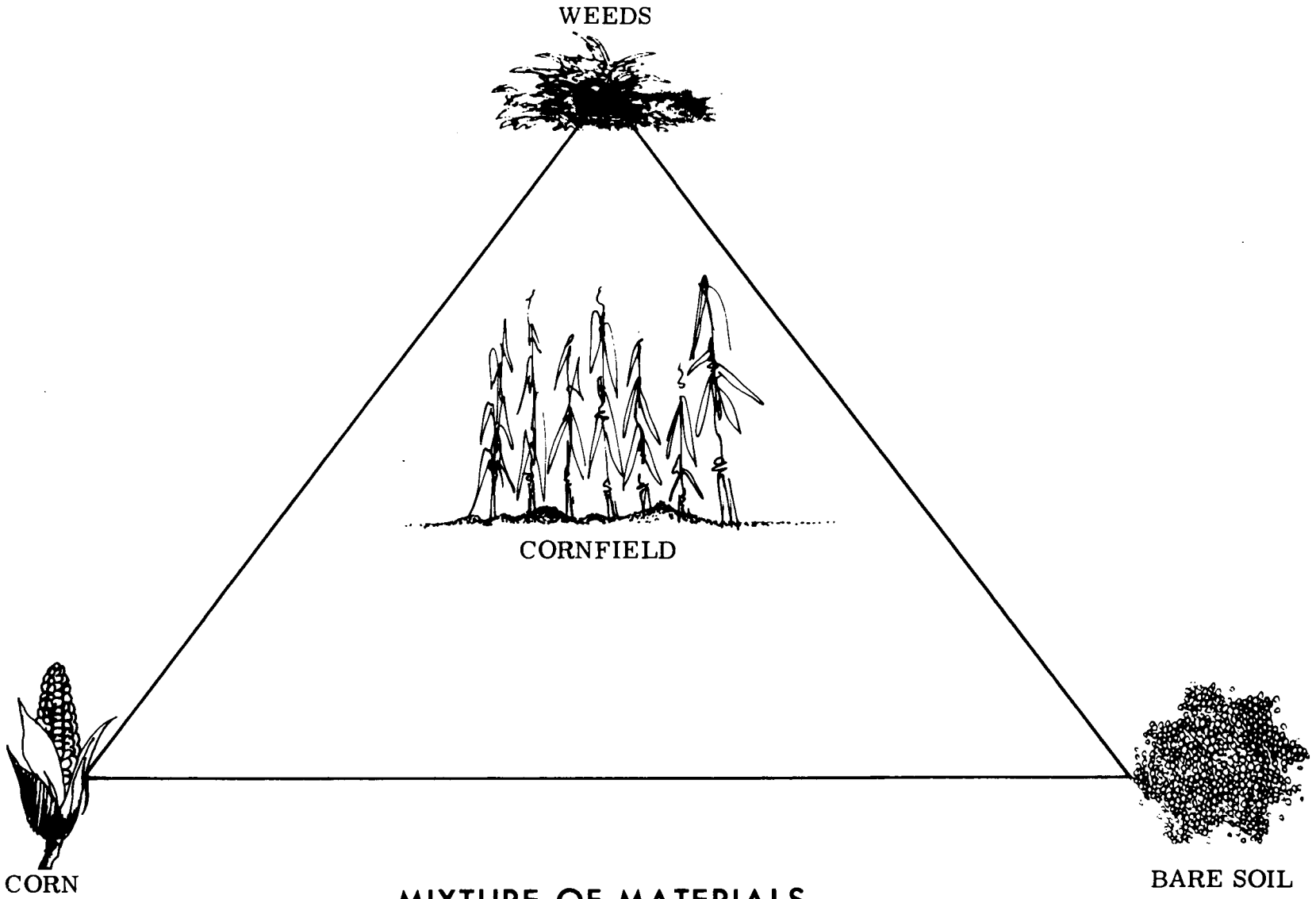

MIXTURE OF MATERIALS

Figure 12

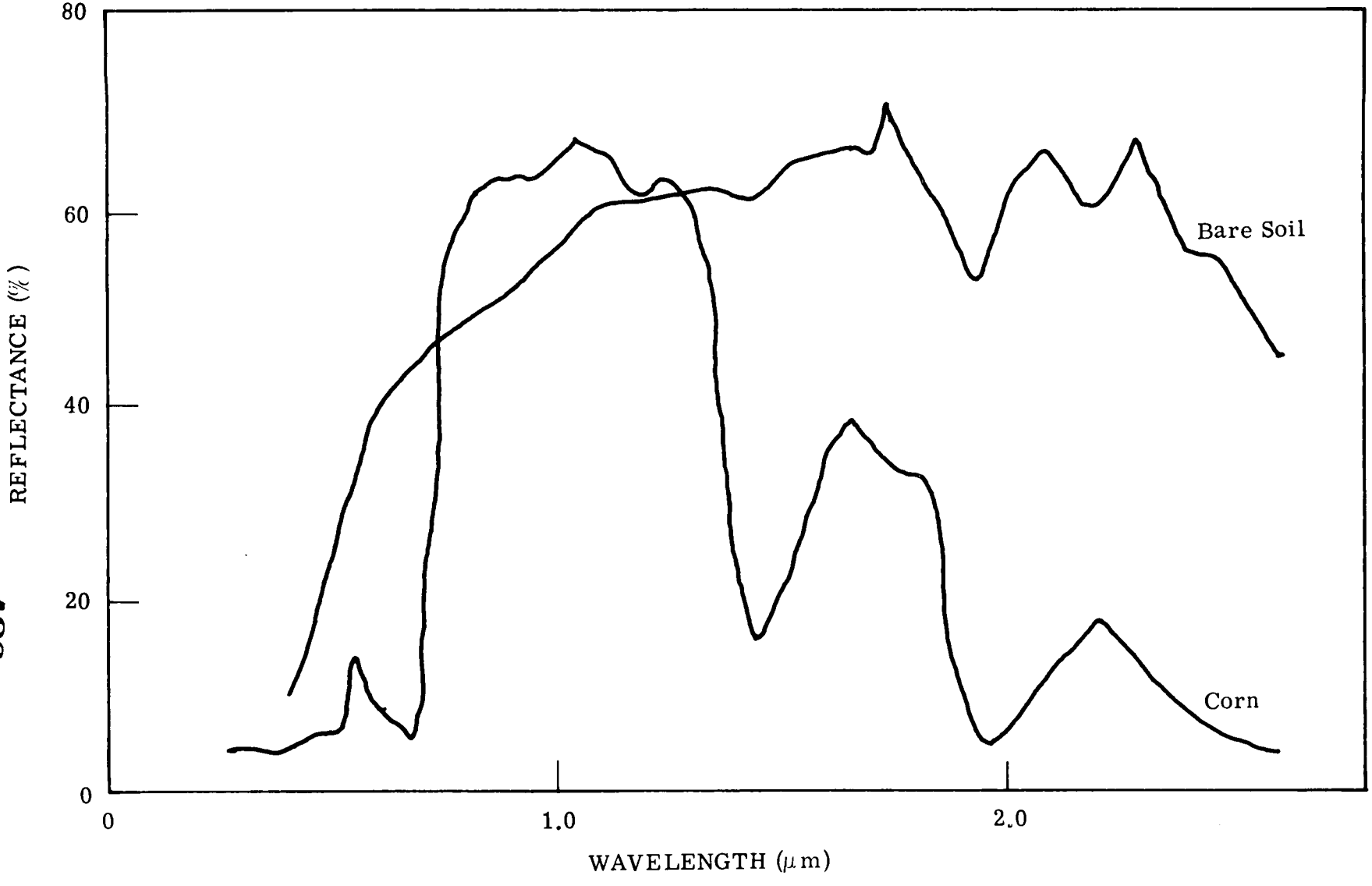

426

REFLECTANCE SPECTRA

Figure 13

INFRARED AND OPTICS LABORATORY
INSTITUTE OF SCIENCE AND TECHNOLOGY
WRL
THE UNIVERSITY OF MICHIGAN

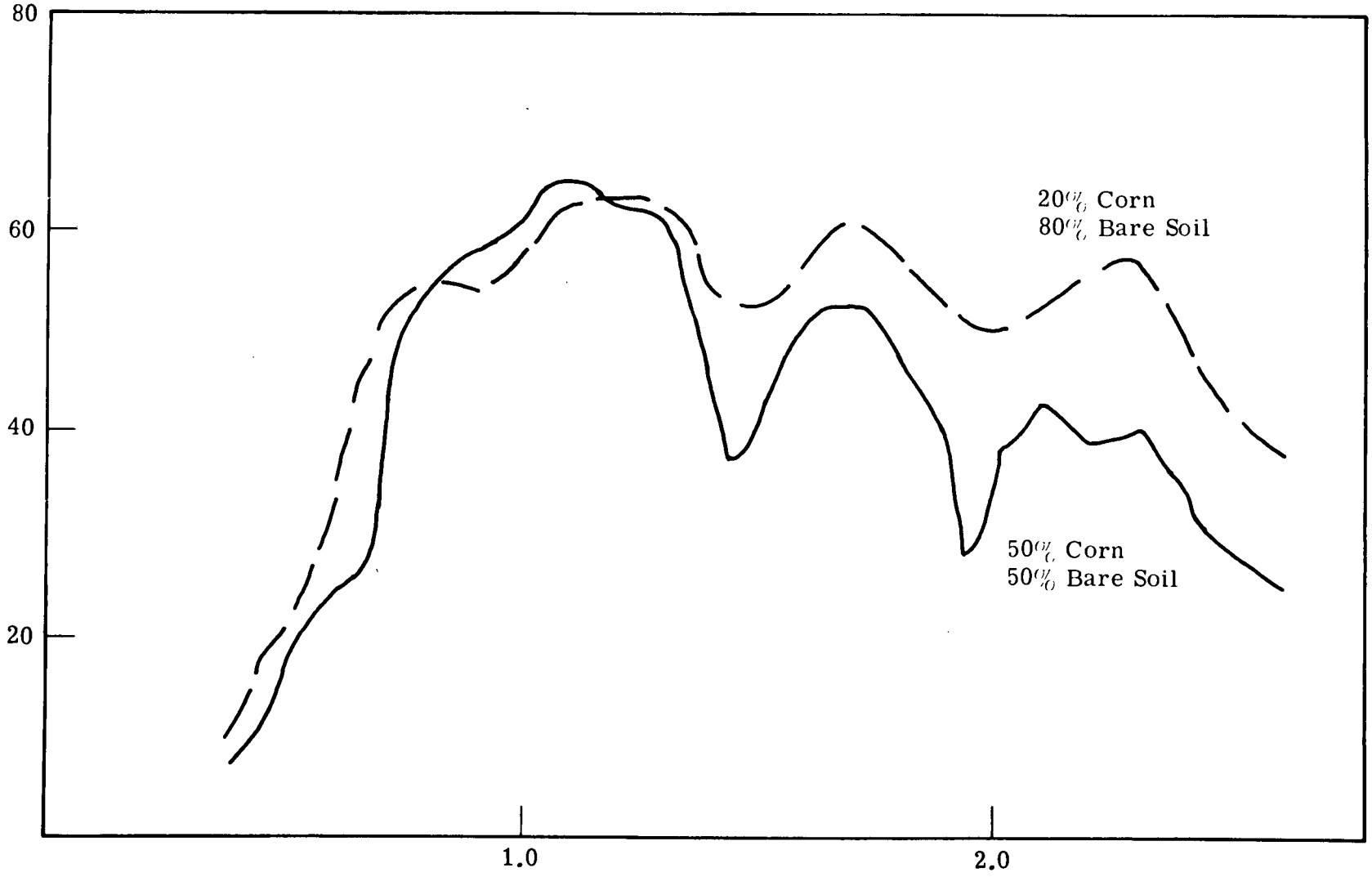

INFRARED AND OPTICS LABORATORY
INSTITUTE OF SCIENCE AND TECHNOLOGY
WRL
THE UNIVERSITY OF MICHIGAN

REFLECTANCE SPECTRA OF MIXTURES

Figure 14

CALCULATED ESTIMATES OF
VEGETATIONAL COMPONENTS OF EXPERIMENTAL PLOTS

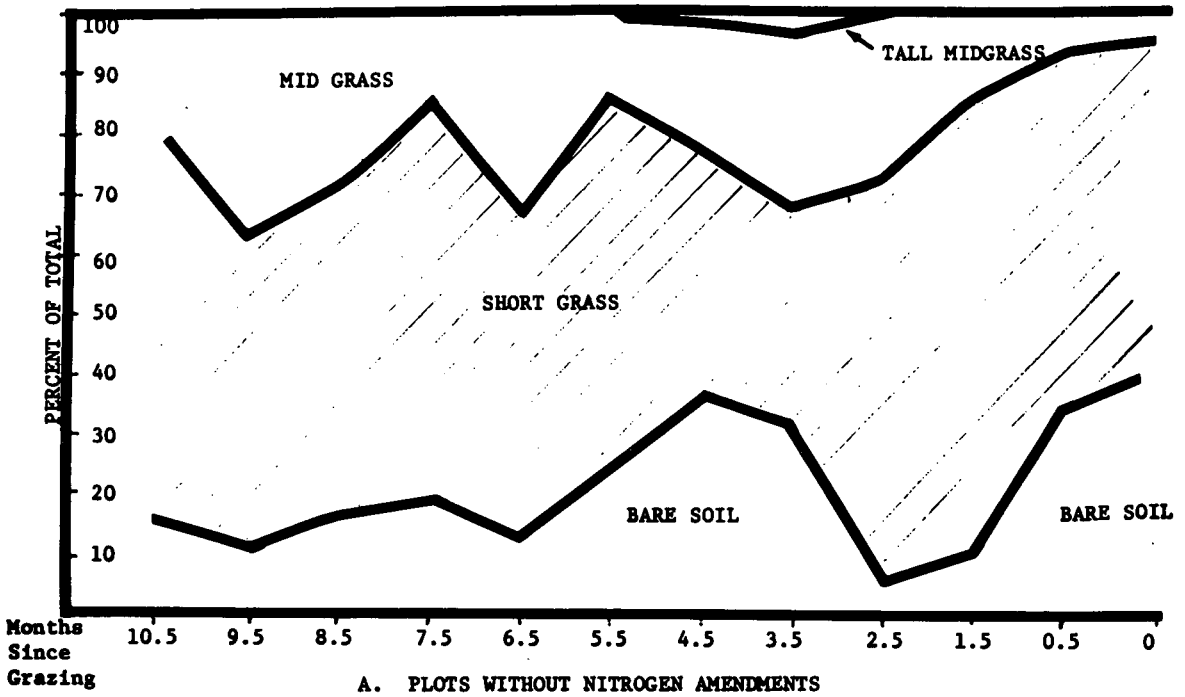

A. PLOTS WITHOUT NITROGEN AMENDMENTS

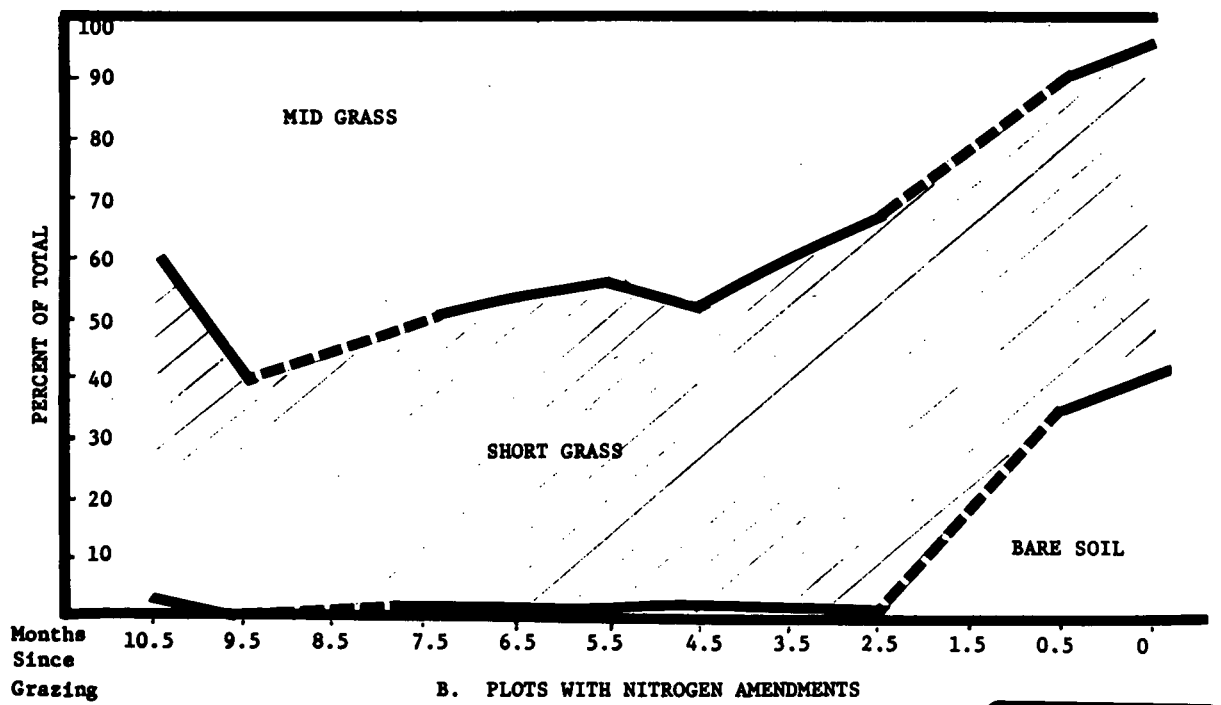

B. PLOTS WITH NITROGEN AMENDMENTS

INFRARED AND OPTICS LABORATORY
INSTITUTE OF SCIENCE AND TECHNOLOGY
WRL
THE UNIVERSITY OF MICHIGAN

Figure 15

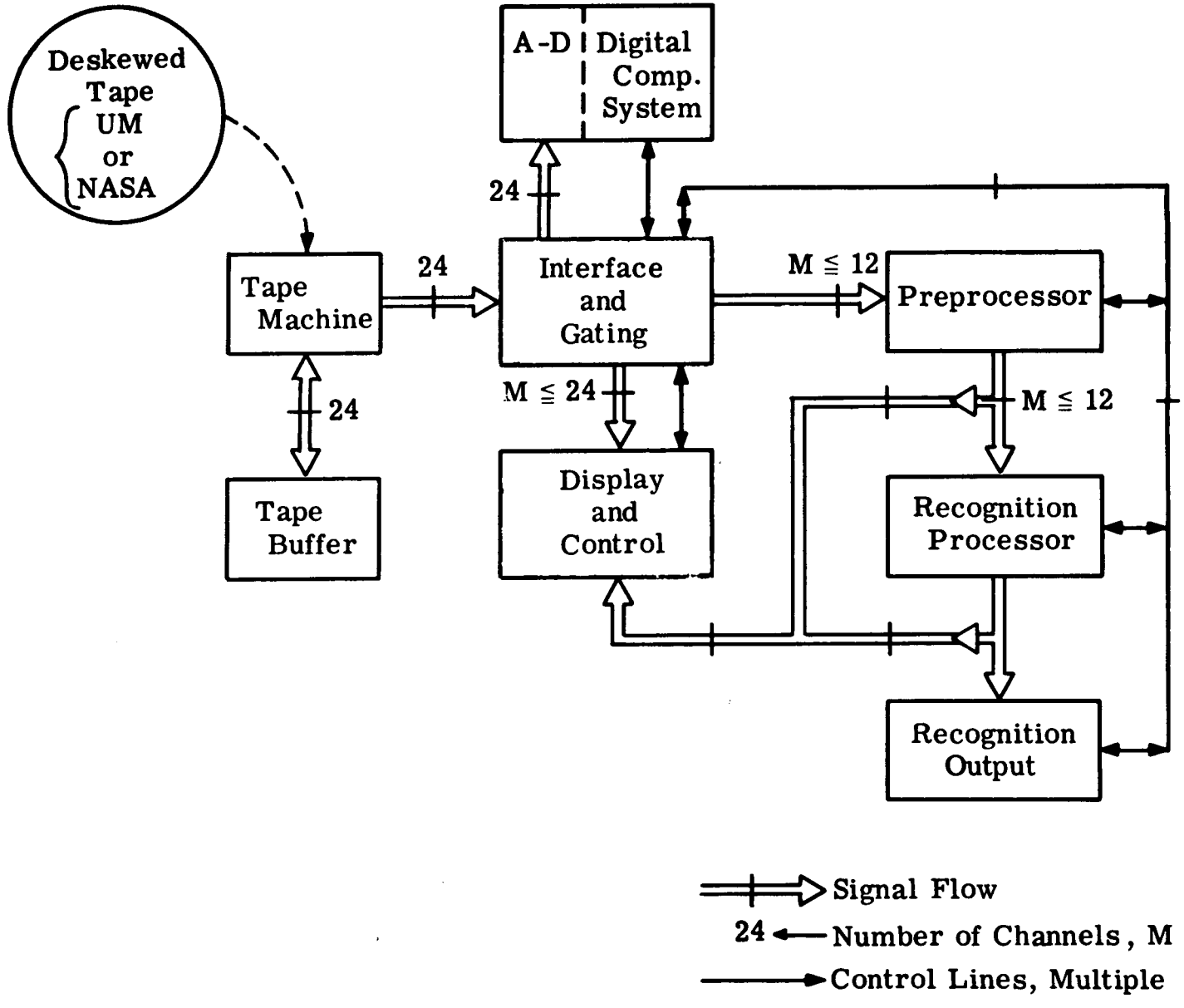

SPECTRAL ADAPTIVE RECOGNITION COMPUTER/HYBRID (SPARC/H)

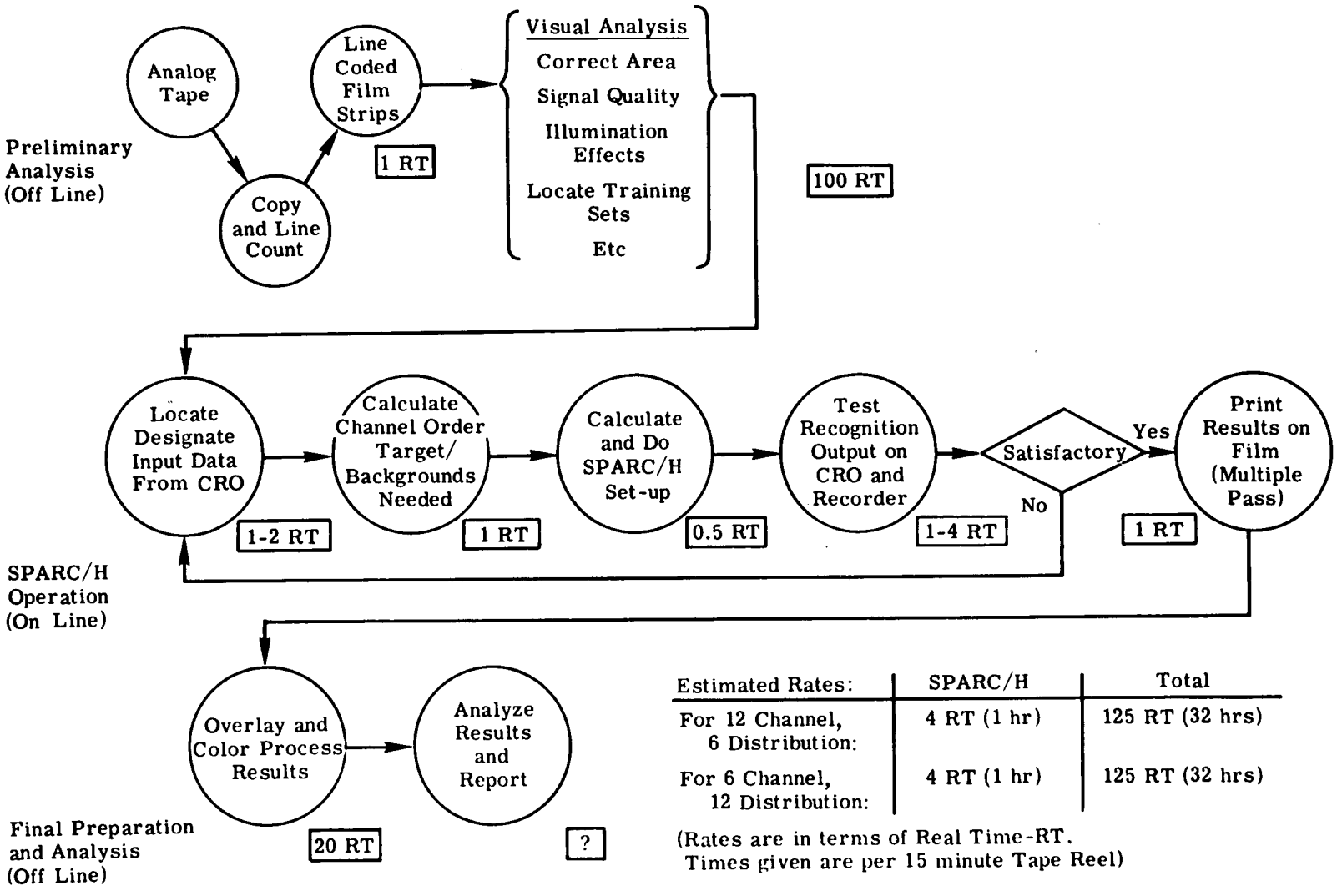

Estimated Rates:	SPARC/H	Total
For 12 Channel, 6 Distribution:	4 RT (1 hr)	125 RT (32 hrs)
For 6 Channel, 12 Distribution:	4 RT (1 hr)	125 RT (32 hrs)

(Rates are in terms of Real Time-RT. Times given are per 15 minute Tape Reel)

SPARC/H PROCESSING FLOW AND TIMING CHART

Figure 17